IEEE Access
Multidisciplinary | Rapid Review | Open Access Journal

SPECIAL SECTION ON EVOLVING TECHNOLOGIES IN ENERGY STORAGE SYSTEMS FOR ENERGY SYSTEMS APPLICATIONS

Received April 22, 2020, accepted May 2, 2020, date of publication May 7, 2020, date of current version May 20, 2020.

Digital Object Identifier 10.1109/ACCESS.2020.2992986

A Compact and Cost Efficient Multiconverter for Multipurpose Applications

MD. HALIM MONDOL[1], MD. SHIHAB UDDIN[1], EKLAS HOSSAIN[2], (Senior Member, IEEE), AND SHUVRA PROKASH BISWAS[1]

[1]Department of Electronics and Telecommunication Engineering, Rajshahi University of Engineering and Technology, Rajshahi 6204, Bangladesh
[2]Oregon Renewable Energy Center (OREC), Department of Electrical Engineering and Renewable Energy, Oregon Institute of Technology, Klamath Falls, OR 97601, USA

Corresponding author: Md. Halim Mondol (halimreza18@gmail.com)

ABSTRACT This paper presents a novel single-phase to single-phase multiconverter topology that can be applied in multiple areas. The proposed multiconverter is designed with only two soft power semiconductor switches (e.g. MOSFET or IGBT), four power diodes and a center-tapped transformer which makes it more compact in size, decrease the gate driving complexity, reduce the total equipment costs and enhance the energy conversion efficiency with minimized losses. Furthermore, the utilization of the transformer in the proposed converter mitigates the multiple AC source requirement problems and provides galvanic isolation which increases the reliability of the converter. Moreover, the presented multiconverter is applicable in various areas including electric traction as a speed controller, induction heating, AC and DC variable power supplies, etc. which signify the competence of this converter in energy conversion appliances. However, a comparative analysis of the offered converter with the existing AC-AC converters is also introduced in this paper with respect to the number of components, equipment costs, gate driving complexity, and application areas. In order to evaluate the performance of the proposed multiconverter, the simulation-based results carried out in MATLAB/Simulink are presented and analyzed in this paper with proper descriptions. Finally, a scaled-down prototype is developed in the laboratory to validate the simulation results and the feasibility of the proposed multiconverter.

INDEX TERMS Cycloconverter, controlled rectifier, electric traction, matrix converter, multiconverter, static frequency changer (SFC), voltage regulator.

I. INTRODUCTION

Generally, the electrical energy generated by the power converters from the renewable energy sources is integrated into the utility grid at a constant frequency which is later distributed to the consumer with the standard value of voltage and frequency. But, there are certain areas where the value of the voltage and it's frequency need to be varied for desired purposes. These areas include speed control of the electric traction motor, high frequency induction heating, AC voltage regulation, and controlled rectifier for variable power supply [1]–[4]. In, electric traction, the frequency of the grid voltage supplied to the input of the motor drive need to be stepped down than the rated frequency of the drive by keeping the voltage at the fixed value to control its speed where the induction heating demands the standard frequency to be stepped up to the required high frequency AC current in order to generate essential heat [5]–[7]. Moreover, in some applications (e.g. variable AC power supply), the value of the standard AC voltage of the grid needs to be controlled which is done by the AC voltage controllers i.e. AC voltage regulators [8]–[10]. Furthermore, the rectified grid voltage is controlled by the controlled rectifier to produce a variable DC power supply. From the aforesaid discussion, it is clear that the standard values of the voltage and the frequency are needed to vary in order to drive certain industrial devices. Thus, many converters are used to convert the standard power supplied by the generation unit to the power of different voltage rating, current rating, and frequency rating according to the requirement of the electrical devices [11]–[13].

The most common converters that are used to change the static voltage and AC frequency to an adjustable range without using further transitional DC links are known as cycloconverters or static frequency changers (SFCs).

The associate editor coordinating the review of this manuscript and approving it for publication was Sanjeevikumar Padmanaban.

Nowadays, the cycloconverters are used as an AC voltage controller [14], static frequency changer [15], controlled rectifier [16], and PWM charger for energy storage systems [17] simultaneously. But, before the invention of the high rated thyristors, cycloconverters were not much familiar in practical and commercial applications. With the advent of the massive rated thyristors as well as the advancement of the microprocessor-based operations, thyristors controlled cycloconverters are now being commonly used in manufacturing industries for applications in electrical traction [18], rolling steel mill [19], SAG mill drive [20].

However, several cycloconverter topologies have been introduced by the researchers in recent years. The most conventional topology [21] structured with hard switching elements (e.g. thyristors) suffers from the complexity of the gate driver circuits, as a negative pulse needs to apply into its gate to turn it OFF forcefully during the operation of high frequency conversion. Moreover, the bridge type topology proposed in [22] which is composed with the combination of two controlled bridge rectifiers interconnected back to back with the load demands higher number of switches that, raises the total equipment costs, increases the overall size and weight of the system, and even the complexity of the gate driving circuits. Another soft switch half wave cycloconverter is addressed in [23], where four MOSFETs are used that increases total conduction losses and even equipment costs. Nevertheless, there are more topologies proposed by the authors including AC-AC matrix converter [24], high-frequency ac link converters [25], variable frequency drive converter (VFD) [26], current source cycloconverter [27], envelope cycloconverter [28] which use an unsatisfactory number of switching components as compared to the conventional cycloconverter in order to enhance the overall performance of the system.

Among the aforesaid converters, the AC-AC matrix converters have also drawn attention significantly and are being used vastly in industry level applications with improved performance. The conventional single phase to single phase PWM ac-ac matrix converters proposed in [29]–[31] are able to change the magnitude of the AC input voltage by varying the duty ratio. Still, they are unable to change the input frequency, although each topology uses four semiconductor switches. These major limitations of the previously mentioned topologies were eradicated by adding a bidirectional phase leg within each topology by the authors of the papers proposed in [32], [33]. Therefore, each of the resultant topology is structured with eight unidirectional switches which significantly increases the total conduction losses, falls down the conversion efficiency, and raises the total equipment costs.

But, the topology presented in [34] focuses on the reduction of total harmonic distortion (THD) from the converted high frequency signal rather than the reduction of switching elements. As a result, this topology provides better output waveforms, but, still produces high conduction losses and demands unsatisfactory amount of equipment costs. Furthermore, the utilization of inductor to generate better sinewave falls down the power factor under effective range. In order to overcome these problems, recently, a new matrix converter topology was offered in [35] with reduced number of switches which is capable of changing the voltage and frequency at a time. Still, it requires six switches causing higher conduction and switching losses and does not offer galvanic isolation resulting in decreased reliability of the equipment. Therefore, these topologies are not commercially attractive because of their large number of switching element requirements and gate driving complexity.

In order to mitigate the limitations discussed above, an advanced and compact cycloconverter topology is proposed in this paper with less number of switching elements and lower complexity in gate driver circuits. Hence, the total equipment costs are minimized significantly and the energy conversion efficiency is enhanced to a satisfactory level. Furthermore, the proposed topology consists of soft switching devices (e.g. MOSFET) and it has zero voltage switching that decreases the switching loss and eradicates commutation problems. Moreover, the offered topology can be operated as a step-up and step-down cycloconverter i.e. matrix converter, AC voltage regulator, and controlled rectifier according to the desired application and thus it is called a multiconverter. Therefore, it is clear that this topology may play an attractive and significant role in commercial applications.

The rest of the paper is organized as follows: the proposed multiconverter topology and its switching scheme are described in section II. The operating principle and calculation of losses are explained in section III and section IV. The simulation based results are demonstrated in section V. Section VI represents the experimental results of the proposed multiconverter to evaluate its performance. Comparison of the proposed topology with some existing topologies is shown in section VII. Finally, the paper is concluded in section VIII.

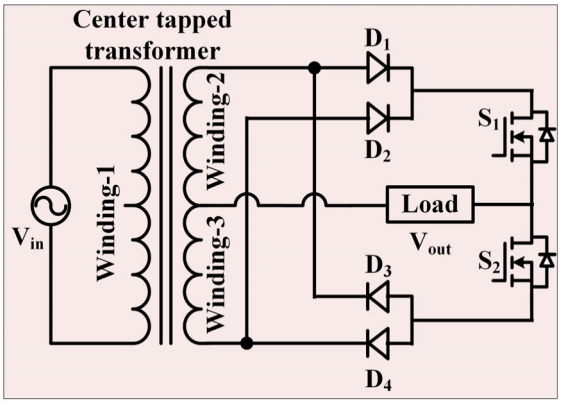

FIGURE 1. Circuit configuration of the proposed multi-converter.

II. PROPOSED MULTICONVERTER AND ITS SWITCHING TECHNIQUE

The circuit configuration of the proposed converter topology is shown in Fig. 1 which is structured with only two soft

semiconductor switching devices (e.g. MOSFET), four power diodes, and a center-tapped transformer. As the switches can be operated according to the desired application with less gate driver complexity, the proposed converter can be used as a multiconverter. Moreover, the utilization of the center trapped transformer provides galvanic isolation that increases the reliability of the circuitry elements and eliminates multiple direct AC source requirements. Thus, the proposed converter is compact, cost-efficient, and reliable simultaneously. However, in the following subsection, the switching technique to operate the multiconverter in variety of applications is explained with necessary diagrams.

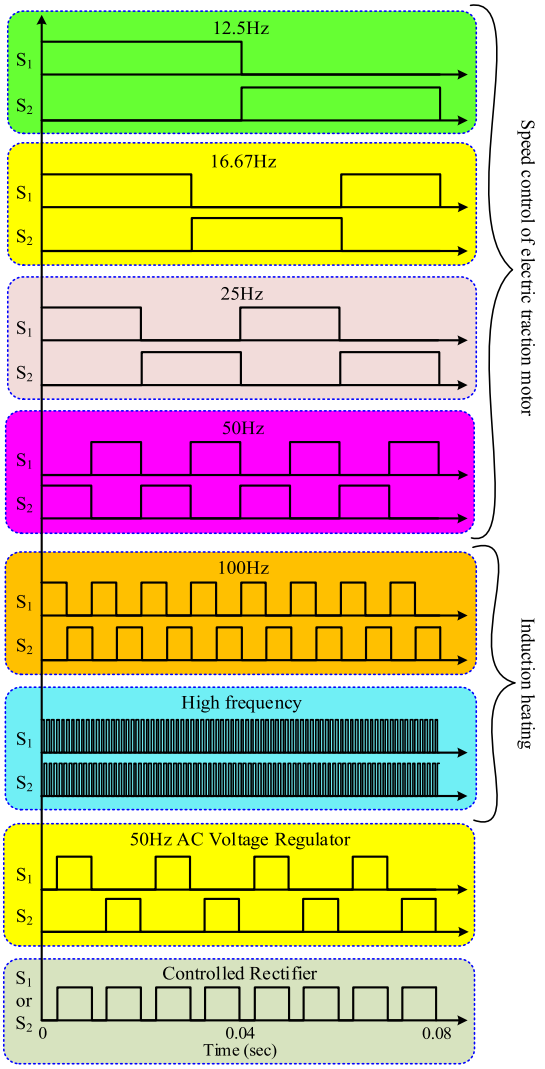

FIGURE 2. Gate driving signals of the proposed multiconverter for different converting modes.

A. SWITCHING TECHNOLOGY

The presented converter is able to be operated as a step-up and step-down cycloconverter, AC voltage regulator and controlled rectifier. The switching pulses to operate this converter as an expected power converter are represented in Fig. 2 with proper explanations. Form Fig. 2, it can be seen that the switching frequency is needed to set at a value that is equivalent to the frequency of the output voltage with 50% duty cycle during the operation as a cycloconverter or SFC. Moreover, the duty cycles of the gate pulses are varied along with the expected value of the output voltage to operate the converter as an AC voltage regulator or a controlled rectifier. In order to operate the proposed converter as a resonant induction heater, the switching frequency is set to a very value and a resonant circuit in connected at the load terminal. However, the switching states of the proposed mulitconverter with respective output voltages are listed in Table 1 for different converting modes.

III. OPERARTING PRINCIPLE

The operating principle of the proposed multiconverter is explained based on the type of active energy conversion modes including step-down cycloconverter, step-up cycloconverter, AC voltage regulator, and controlled rectifier. However, there are four common working modes of this converter during all of the active conversion modes which are shown in Fig. 3. Thus, the explanation of these four working modes help to understand the operating principle of the proposed converter as any of the aforesaid converter. The four working modes are described as follows:

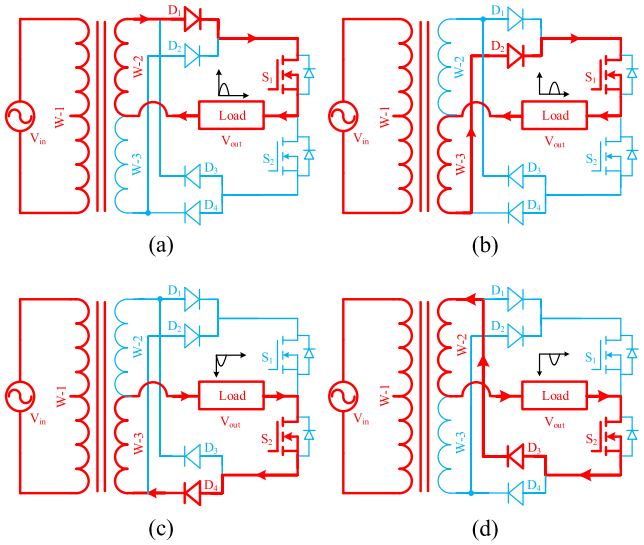

FIGURE 3. Generalized active working modes of the proposed multiconverter (a) mode-1, (b) mode-2, (c) mode-3, and (d) mode-4.

Mode-1: In this mode, winding-2 of the transformer, switch S_1, and diode D_1 provide conduction path to flow the current through the load which is shown in Fig. 3(a). Thus, the polarity of the output voltage remains similar to the input voltage which is,

$$V_{out} = V_{in} \tag{1}$$

Mode-2: Switch S_1 and diode D_2 are ON state during this mode. Hence, the negative input voltage is transferred to

TABLE 1. Switching states of the multiconverter with respective output voltages for different energy conversion modes.

Energy conversion modes	Output frequency (Hz)	Active transformer winding	Switching states (ON = 1, OFF = 0)						Output voltage (V_{out})	Ranges of θ
			S_1	S_2	D_1	D_2	D_3	D_4		
Step-down cycloconverter	12.5	2	1	0	1	0	0	0	$V_m sin\theta$	$(0 \le \theta \le \pi)$, $(2\pi \le \theta \le 3\pi)$
			0	1	0	0	1	0	$V_m sin\theta$	$(5\pi \le \theta \le 6\pi)$, $(7\pi \le \theta \le 8\pi)$
		3	1	0	0	1	0	0	$-V_m sin\theta$	$(\pi \le \theta \le 2\pi)$, $(3\pi \le \theta \le 4\pi)$
			0	1	0	0	0	1	$-V_m sin\theta$	$(4\pi \le \theta \le 5\pi)$, $(6\pi \le \theta \le 7\pi)$
	16.67	2	1	0	1	0	0	0	$V_m sin\theta$	$(0 \le \theta \le \pi)$, $(2\pi \le \theta \le 3\pi)$
			0	1	0	0	1	0	$V_m sin\theta$	$(3\pi \le \theta \le 4\pi)$, $(5\pi \le \theta \le 6\pi)$
		3	1	0	0	1	0	0	$-V_m sin\theta$	$(\pi \le \theta \le 2\pi)$
			0	1	0	0	0	1	$-V_m sin\theta$	$(4\pi \le \theta \le 5\pi)$
	25	2	1	0	1	0	0	0	$V_m sin\theta$	$(0 \le \theta \le \pi)$
			0	1	0	0	0	1	$V_m sin\theta$	$(3\pi \le \theta \le 4\pi)$
		3	0	1	0	0	1	0	$-V_m sin\theta$	$(2\pi \le \theta \le 3\pi)$
			1	0	0	1	0	0	$-V_m sin\theta$	$(\pi \le \theta \le 2\pi)$
Operating at f_{in}	50	2	1	0	1	0	0	0	$V_m sin\theta$	$(0 \le \theta \le \pi)$
			0	1	0	0	1	0	$V_m sin\theta$	$(\pi \le \theta \le 2\pi)$
Step-up cycloconverter	100	2	1	0	1	0	0	0	$V_m sin\theta$	$(0 \le \theta \le \pi/2)$
			0	1	0	0	1	0	$-V_m sin\theta$	$(\pi/2 \le \theta \le \pi)$
		3	1	0	0	1	0	0	$-V_m sin\theta$	$(\pi \le \theta \le 3\pi/2)$
			0	1	0	0	0	1	$V_m sin\theta$	$(3\pi/2 \le \theta \le 2\pi)$
AC voltage regulator	50	2	1	0	1	0	0	0	$V_m sin\theta$	$(\alpha \le \theta \le \pi)$
			0	1	0	0	1	0	$V_m sin\theta$	$(\pi+\alpha \le \theta \le 2\pi)$
Controlled rectifier	0	2	1	0	1	0	0	0	$V_m sin\theta$	$(\beta \le \theta \le \pi)$
		3	1	0	0	1	0	0	$-V_m sin\theta$	$(\pi+\beta \le \theta \le 2\pi)$

the load by the transformer winding-3 using the conduction path created by S_1 and D_2 which is depicted in Fig. 3(b). So, the output voltage is,

$$V_{out} = -V_{in} \tag{2}$$

Mode-3: During this mode represented in Fig. 3(c), switch S_2, diode D_4 and transformer winding-3 are used to apply the positive input voltage from the opposite direction to the load. Therefore, the output voltage becomes,

$$V_{out} = -V_{in} \tag{3}$$

Mode-4: In this mode, switch S_2, diode D_3 and transformer winding-2 create active conducting path for the load current from same direction as mode-3 which is illustrated in Fig. 3(d). Consequently, the output voltage becomes equivalent to the input voltage. That is

$$V_{out} = V_{in} \tag{4}$$

Nevertheless, the working principle of the proposed multiconverter is described according to the individual active energy conversion mode in the following subsections.

A. PROPOSED TOPOLOGY AS A STEP-DOWN CYCLOCONVERTER

Generally, the step-down cycloconverter provides an output voltage of frequency less than the frequency of the input voltage. The presented converter can be operated to convert the input frequency to its half, one-third, and one-fourth output frequency as a step-down cycloconverter. More likely, if the input voltage frequency is 50Hz, it can produce output voltage of 25Hz, 16.67Hz, and 12.5Hz. Thus, the working principle to produce required output frequency are as follows:

1) 25Hz

During the positive half cycle of the output voltage, there are two states. Mode-1 and mode-2 (illustrated in Fig. 3(a) and Fig. 3(b)) take place during state-1 and state-2 respectively as shown in Fig. 4. Thus, the respective output voltages are,

$$V_{out} = V_m \sin\theta; \quad 0 \le \theta \le \pi \tag{5}$$

$$V_{out} = -V_m \sin\theta; \quad \pi \le \theta \le 2\pi \tag{6}$$

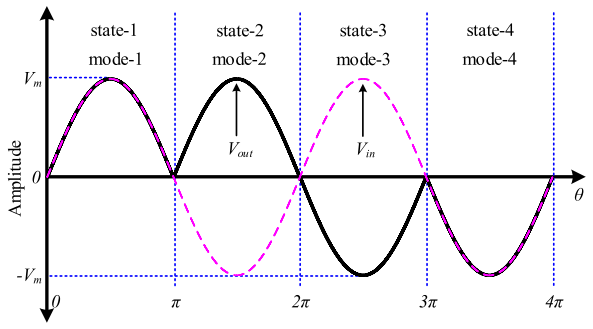

FIGURE 4. Operating states of the converter as a step-down cycloconverter with the respective working modes to generate 25Hz output frequency.

Here, V_m is the peak amplitude of the input voltage. Moreover, during the negative half cycle of the output voltage depicted in Fig. 4, state-3 and state-4 are obtained from the working mode-3 and mode-4 (represented in Fig. 3(c) and Fig. 3(d)). Hence, the output voltages within state-3 and state-4 are,

$$V_{out} = -V_m \sin\theta; \quad 2\pi \le \theta \le 3\pi \tag{7}$$

$$V_{out} = V_m \sin\theta; \quad 3\pi \le \theta \le 4\pi \tag{8}$$

2) 16.67Hz

There are three states that occur during the positive half cycle of the output voltage. The working mode-1 is repeated to generate state-1 and state-3 where state-2 is achieved from operating the converter at working mode-2 as shown in Fig. 5. Hence, the output voltage within state-1, state-2 and state-3 are,

$$V_{out} = V_m \sin\theta; \quad 0 \le \theta \le \pi \tag{9}$$
$$V_{out} = -V_m \sin\theta; \quad \pi \le \theta \le 2\pi \tag{10}$$
$$V_{out} = V_m \sin\theta; \quad 2\pi \le \theta \le 3\pi \tag{11}$$

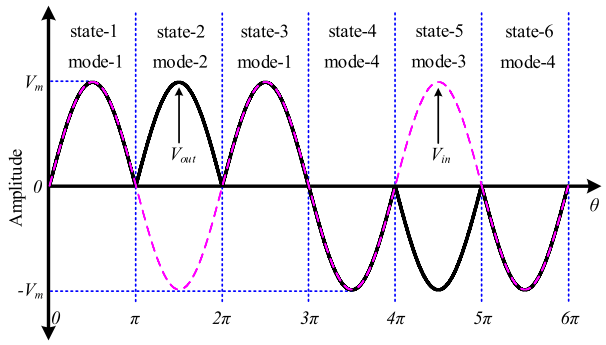

FIGURE 5. Operating states of the converter as a step-down cycloconverter with the respective working modes to generate 16.67Hz output frequency.

However, state-4 and state-6 are originated by operating the proposed converter at mode-4. Further, mode-3 helps to obtain state-6 during the negative half cycle of the output voltage which is shown in Fig. 5. Therefore, the output voltage achieved during state-4, state-5 and state-6 are,

$$V_{out} = V_m \sin\theta; \quad 3\pi \le \theta \le 4\pi \tag{12}$$
$$V_{out} = -V_m \sin\theta; \quad 4\pi \le \theta \le 5\pi \tag{13}$$
$$V_{out} = V_m \sin\theta; \quad 5\pi \le \theta \le 6\pi \tag{14}$$

3) 12.5Hz

There are attained total eight states as shown in Fig. 6 while operating the proposed converter in the generation of 12.5Hz output frequency. During the positive half cycle of the output voltage, state-1 and state-3 are generated by applying mode-1 where mode-2 is used twice to produce state-2 and state-4. Thus, the resultant output voltage obtained from state-1 to state-4 can be expressed as,

$$V_{out} = V_m \sin\theta; \quad 0 \le \theta \le \pi \tag{15}$$
$$V_{out} = -V_m \sin\theta; \quad \pi \le \theta \le 2\pi \tag{16}$$
$$V_{out} = V_m \sin\theta; \quad 2\pi \le \theta \le 3\pi \tag{17}$$
$$V_{out} = -V_m \sin\theta; \quad 3\pi \le \theta \le 4\pi \tag{18}$$

Furthermore, state-5 and state-7 are achieved from the application of the active working mode-3. Moreover, mode-4 is the reason behind the generation of state-6 and state-8 within the negative half cycle of the output voltage. The corresponding

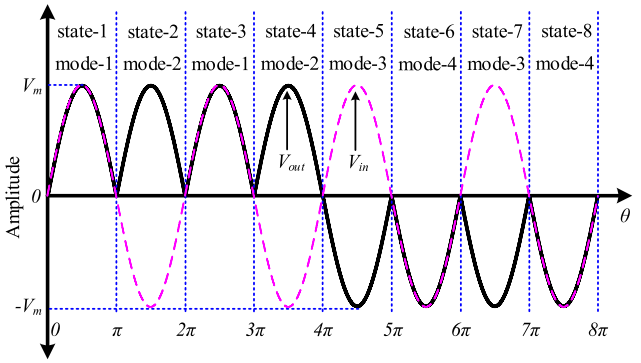

FIGURE 6. Operating states of the converter as a step-down cycloconverter with the respective working modes to generate 12.5Hz output frequency.

output voltages during state-5 to state-8 are written in the following equations.

$$V_{out} = -V_m \sin\theta; \quad 4\pi \le \theta \le 5\pi \tag{19}$$
$$V_{out} = V_m \sin\theta; \quad 5\pi \le \theta \le 6\pi \tag{20}$$
$$V_{out} = -V_m \sin\theta; \quad 6\pi \le \theta \le 7\pi \tag{21}$$
$$V_{out} = V_m \sin\theta; \quad 7\pi \le \theta \le 8\pi \tag{22}$$

B. PROPOSED TOPOLOGY AS A STEP-UP CYCLOCONVERTER

When the frequency of the input voltage is needed to increase for certain applications such as induction heating, step-down cycloconverter is used. A high frequency resonant circuit can heat a body situated within its range. The higher the frequency, the larger amount of heat is induced. Thus, the step-up cycloconverter is suitable for induction heating. However, the operating principle of the proposed multiconverter as a step-up cycloconverter is explained for generating the output frequency twice of the input i.e. 100Hz, for ease of understanding. But, this converter can be easily used to generate higher output frequency taking account the switching loss within an acceptable range which is quite difficult using hard switches such as thyristors, as the gate driving complexity increases unsatisfactorily. Nevertheless, the working functions of the offered converter as a step-up cycloconverter are as follows:

During the positive half cycle of the input voltage, active working mode-1 and mode-2 are applied according to the gate pulses shown in Fig. 2 for 100Hz in order to generate state-1 and state-2 respectively. Thus, the respective output voltages of these two states which are shown in Fig. 7 can be denoted as,

$$V_{out} = V_m \sin\theta; \quad 0 \le \theta \le \pi/2 \tag{23}$$
$$V_{out} = -V_m \sin\theta; \quad \pi/2 \le \theta \le \pi \tag{24}$$

However, state-3 and state-4 are produced by applying the active working mode-3 and mode-4 respectively during the negative half cycle of the input voltage as illustrated in Fig. 7.

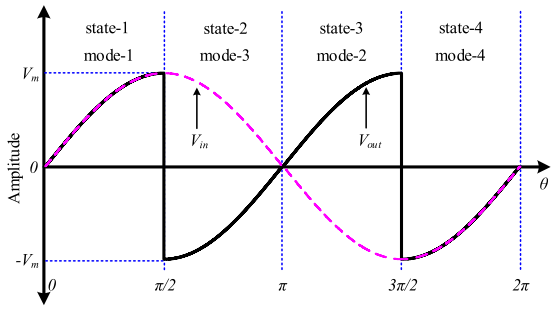

FIGURE 7. Operating states of the converter as a step-up cycloconverter with the respective working modes to generate 100Hz output frequency.

Therefore, the output voltages at this two states stand with,

$$V_{out} = V_m \sin\theta; \quad \pi \le \theta \le 3\pi/2 \tag{25}$$

$$V_{out} = -V_m \sin\theta; \quad 3\pi/2 \le \theta \le 2\pi \tag{26}$$

C. PROPOSED TOPOLOGY AS AN AC VOLTAGE REGULATOR

In order to control the RMS value of the input voltage by keeping the frequency constant, the AC voltage controller i.e. AC voltage regulator is used. The proposed converter can be operated at the input frequency to control the input voltage according to the switching pulses shown in Fig. 2. For soft switches such as MOSFETs or IGBTs, the duty cycle D and the delay angle α are considered as the control inputs. Where the duty cycle can be determined from the following equation,

$$D = \frac{\left(t_{on} - \frac{\alpha T}{4\pi}\right)}{t_{on} + t_{off}} \tag{27}$$

Here, t_{on} and t_{off} denote the on-time and off-time within an entire switching cycle T. If the frequency of the input voltage is considered as 50Hz (i.e. $T = 20ms$), then, the maximum value of t_{on} must not exceed 10ms to avoid short circuit. The delay angle α is varied to control the duty cycle of the applied pulses as well as the RMS output voltage. However, in this subsection, the operating principle of the proposed converter as an AC voltage controller is described as follows:

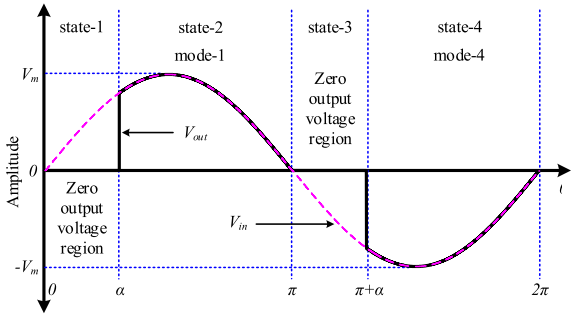

FIGURE 8. Operating states of the proposed converter as an AC voltage regulator with the respective working modes.

There are four states within an entire cycle of the output voltage as shown in Fig. 8. State-1 and state-3 are defined as zero voltage regions caused by the OFF state of the switches and occur during the positive and negative half cycle of the output voltage respectively. The duration of these zero voltage regions depends upon the delay angle α. Nevertheless, state-2 and state-4 are generated using active working mode-1 and mode-4 respectively. Thus, the output voltage during state-2 and state-4 can be expressed as,

$$V_{out} = V_m \sin\theta; \quad \alpha \le \theta \le \pi \tag{28}$$

$$V_{out} = V_m \sin\theta; \quad \pi + \alpha \le \theta \le 2\pi \tag{29}$$

Moreover, the resultant controlled RMS output voltage can be calculated by the following equation [36],

$$V_{out(rms)} = \sqrt{\frac{1}{2\pi}\left(\int_{\alpha}^{\pi} (V_m \sin\theta)^2 \, d\theta + \int_{\pi+\alpha}^{2\pi} (V_m \sin\theta)^2 \, d\theta\right)} \tag{30}$$

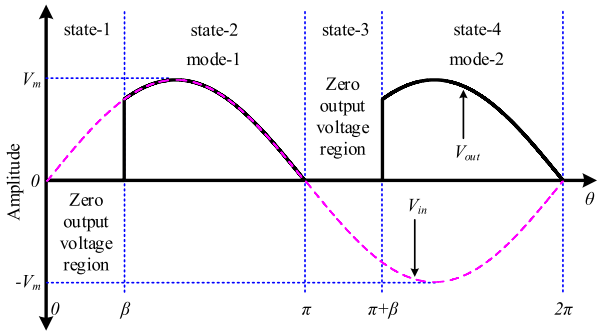

FIGURE 9. Operating states of the proposed converter as a full wave controlled rectifier with the respective working modes.

D. PROPOSED TOPOLOGY AS A FULL WAVE CONTROLLED RECTIFIER

During the operation of the proposed converter as a controlled rectifier, state-2 and state-4 are achieved by applying the active working mode-1 and mode-2 respectively as represented in Fig. 9. The zero voltage regions (i.e. state-1 and state-3) are defined by the control angle β during both positive and negative half cycle of the input voltage. The duty cycle for controlling the rectified average voltage can be determined using the following equation,

$$D = 1 - \frac{\beta}{\pi}; \quad 0 \le \beta \le \pi \tag{31}$$

It should be noted that the switch S_2 needs to be disconnected during this operation to avoid reverse current flow through the body diode. Furthermore, the aforesaid operation can be performed by applying mode-3 and mode-4 while disconnecting the S_1 switch. However, the obtained output voltage at state-2 and state-4 can be written as,

$$V_{out} = V_m \sin\theta; \quad \beta \le \theta \le \pi \tag{32}$$

$$V_{out} = -V_m \sin\theta; \quad \pi + \beta \le \theta \le 2\pi \tag{33}$$

Therefore, the average DC output voltage of the full-wave controlled rectifier is calculated as,

$$V_{out(avg)} = \frac{1}{2\pi}\left(\int_{\beta}^{\pi} V_m \sin\theta d\theta + \int_{\pi+\beta}^{2\pi} V_m \sin\theta d\theta\right) \quad (34)$$

IV. CALCULTAION OF LOSSES

The proposed mulitconverter mainly introduces three type losses including conduction loss (P_C), switching loss (P_S) and the losses produced by the transformer. The losses occurred due to the transformer action are of fixed amount for all the cases which are correlated to the manufacturing process. Thus, the major sources of power losses including conduction loss and switching losses are calculated in the following subsections by ignoring the transformer loss.

A. CONDUCTION LOSSES (P_C)

The conduction losses within a system are caused by the parasitic impedances of the circuit elements including the internal on-state resistances of the switches (R_{sw_on}) and the diodes (R_{D_on}). Thus, the conduction losses occurred by the parasitic resistances of the switches and diodes can be calculated using the following equations [37],

$$P_{C\_sw} = V_{sw\_on}.I_{sw\_avg} + R_{sw\_on}.I^2_{sw\_rms} \quad (35)$$

$$P_{C\_D} = V_{D\_on}.I_{D\_avg} + R_{D\_on}.I^2_{D\_rms} \quad (36)$$

Here, in the above equations, the average current through the switches and diodes are represented by I_{sw_avg} and I_{D_avg} respectively. Moreover, I_{sw_rms} and I_{D_rms} define the RMS currents through the switches and the diodes respectively which are equivalent to the RMS load currents.

However, the conduction losses of the proposed multiconverter significantly vary according to the RMS load current. Thus, the process of calculating the conduction losses with the respective energy conversion modes are as follows:

1) STEP-DOWN CYCLOCONVERTER

For generating 25Hz output frequency, a single switch and a single diode conduct simultaneously during each of the four states within an entire period of the output voltage as shown in Fig. 3 and Fig. 4 respectively. Hence, the conduction losses for this conversion mode can be determined as,

$$P_{C\_25} = 4\left(V_{sw\_on}.I_{sw\_avg} + R_{sw\_on}.I^2_{sw\_rms}\right) + 4\left(V_{D\_on}.I_{D\_avg} + R_{D\_on}.I^2_{D\_rms}\right) \quad (37)$$

Similarly, there are six states within a full cycle of the 16.67Hz output voltage, each of which is generated by the participation of a switch and a diode resulting conduction losses as,

$$P_{C\_16.67} = 6\left(V_{sw\_on}.I_{sw\_avg} + R_{sw\_on}.I^2_{sw\_rms}\right) + 6\left(V_{D\_on}.I_{D\_avg} + R_{D\_on}.I^2_{D\_rms}\right) \quad (38)$$

Moreover, the eight states produced by the eight pairs of switch and diode during each period of the 12.5Hz output voltage produce conduction losses that can be expressed as,

$$P_{C\_12.5} = 8\left(V_{sw\_on}.I_{sw\_avg} + R_{sw\_on}.I^2_{sw\_rms}\right) + 8\left(V_{D\_on}.I_{D\_avg} + R_{D\_on}.I^2_{D\_rms}\right) \quad (39)$$

2) STEP-UP CYCLOCONVERTER

Basically, two switches and two diodes are used to produce the two states within a complete period of 100Hz output voltage. Thus, the conduction losses at 100Hz output frequency are obtained as,

$$P_{C\_100} = 2\left(V_{sw\_on}.I_{sw\_avg} + R_{sw\_on}.I^2_{sw\_rms}\right) + 2\left(V_{D\_on}.I_{D\_avg} + R_{D\_on}.I^2_{D\_rms}\right) \quad (40)$$

3) AC VOLTAGE REGULATOR

The frequency of the output voltage of an AC voltage regulator remains unchanged while the RMS and average output voltages are controlled using two switches and two diodes as described in the previous section. Therefore, the total conduction losses occurred during the operation of the proposed converter as a 50Hz AC voltage regulator can be determined using the following equation,

$$P_{C\_ACVR} = 2\left(V_{sw\_on}.I_{sw\_avg} + R_{sw\_on}.I^2_{sw\_rms}\right) + 2\left(V_{D\_on}.I_{D\_avg} + R_{D\_on}.I^2_{D\_rms}\right) \quad (41)$$

4) CONTROLLED RECTIFIER

From Fig. 3 and Fig. 9, it is can be observed that a single pair of switch and diode are used twice during each cycle of the input voltage to produce the controlled and rectified output voltage. Hence, the total conduction losses introduced by the converter within every cycle of the input voltage during this operation can be calculated as follows,

$$P_{C\_CR} = 2\left(V_{sw\_on}.I_{sw\_avg} + R_{sw\_on}.I^2_{sw\_rms}\right) + 2\left(V_{D\_on}.I_{D\_avg} + R_{D\_on}.I^2_{D\_rms}\right) \quad (42)$$

Therefore, the conduction losses for all of the aforesaid active energy conversion modes can be determined from the above analysis. In the following subsection, the switching loss calculation process is described.

B. SWITCHING LOSSES (P_S)

In practice, the switching delays including turn-on delay (t_{on}) and turn-off delay (t_{off}) associated with the semiconductor devices cause significant amount of power losses due to the overlapping of the off-state voltage and current during the transition periods. Therefore, the power losses occurred during the turn-on and turn-off processes are calculated using

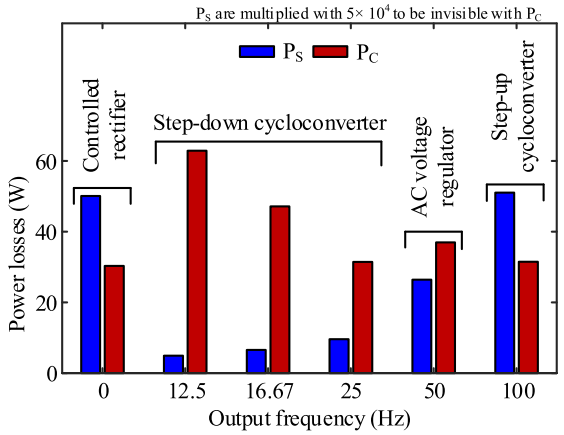

FIGURE 10. Power loss profile of the proposed multiconverter for each of the active energy conversion modes.

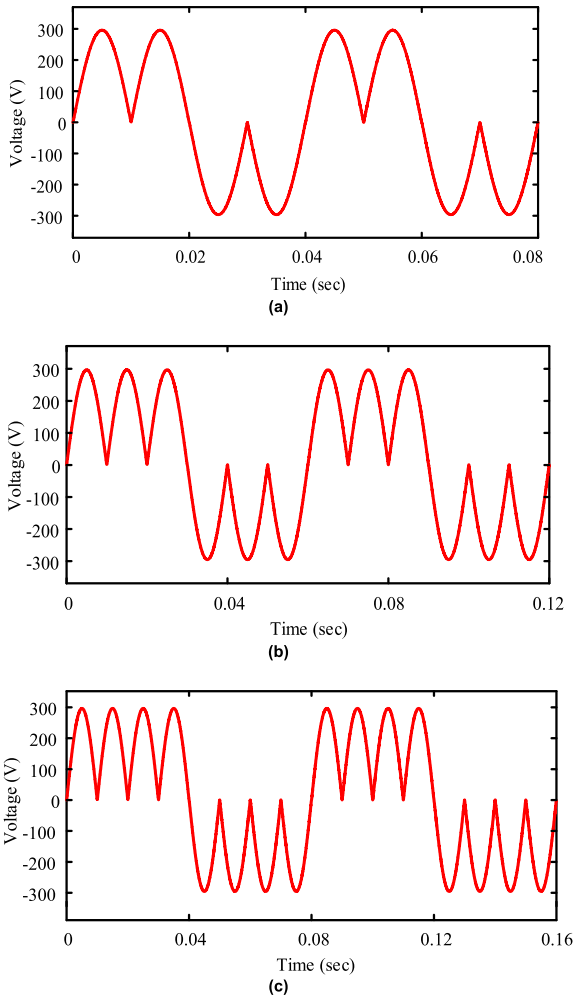

FIGURE 11. Output voltage of the proposed converter as a step-down cycloconverter, (a) 25Hz, (b) 16.67Hz and (c) 12.5Hz.

the following equations [38]:

$$P_{S\_on,m} = f_{sw}\int_0^{t_{on}} v_{off,m}(t).i(t)dt$$

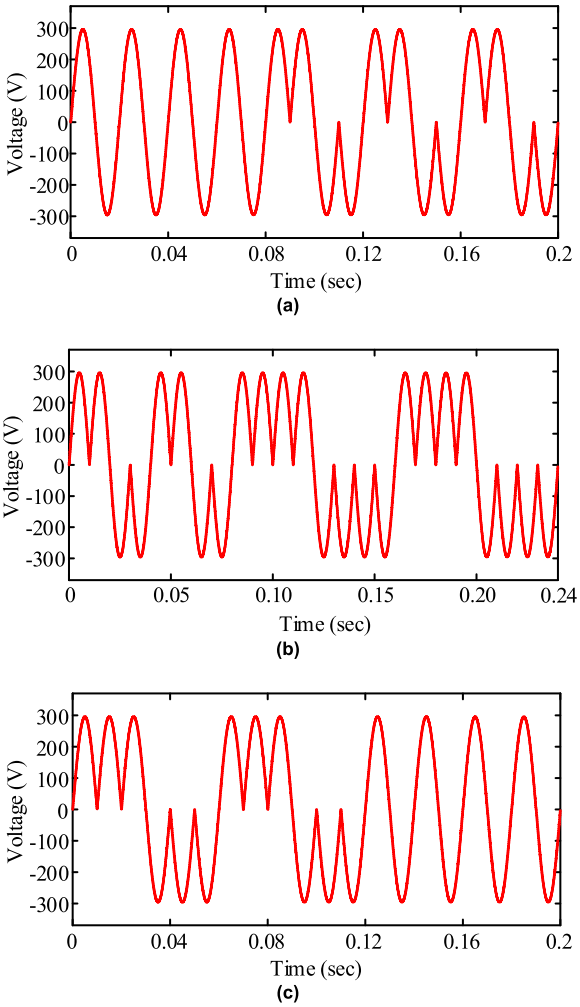

FIGURE 12. Responses of the proposed converter as a step-down cycloconverter during changing output frequency dynamically, (a) 50Hz to 25Hz, (b) 25Hz to 12.5Hz and (c) 16.67Hz to 50Hz.

$$= f_{sw}\int_0^{t_{on}} \left(-\frac{V_{off,m}}{t_{on}}\right)\left(\frac{I_{on1,m}}{t_{on}}(t-t_{on})\right)dt$$

$$= \frac{1}{6}f_{sw}V_{off,m}I_{on1,m}t_{on} \quad (43)$$

$$P_{S\_off,m} = f_{sw}\int_0^{t_{off}} v_{off,m}(t).i(t)dt$$

$$= f_{sw}\int_0^{t_{off}} \left(-\frac{V_{off,m}}{t_{off}}t\right)\left(\frac{I_{on2,m}}{t_{off}}(t-t_{off})\right)dt$$

$$= \frac{1}{6}f_{sw}V_{off,m}I_{on2,m}t_{off} \quad (44)$$

where, the off-state voltage of m^{th} switch is denoted by V_{off} and f_{sw} defines the switching frequency. The on-state currents of m^{th} switch, I_{on1} and I_{on2} represent the currents when the switch is completely turned-on and before the turned-off state respectively. Thus, the total switching loss of a system is

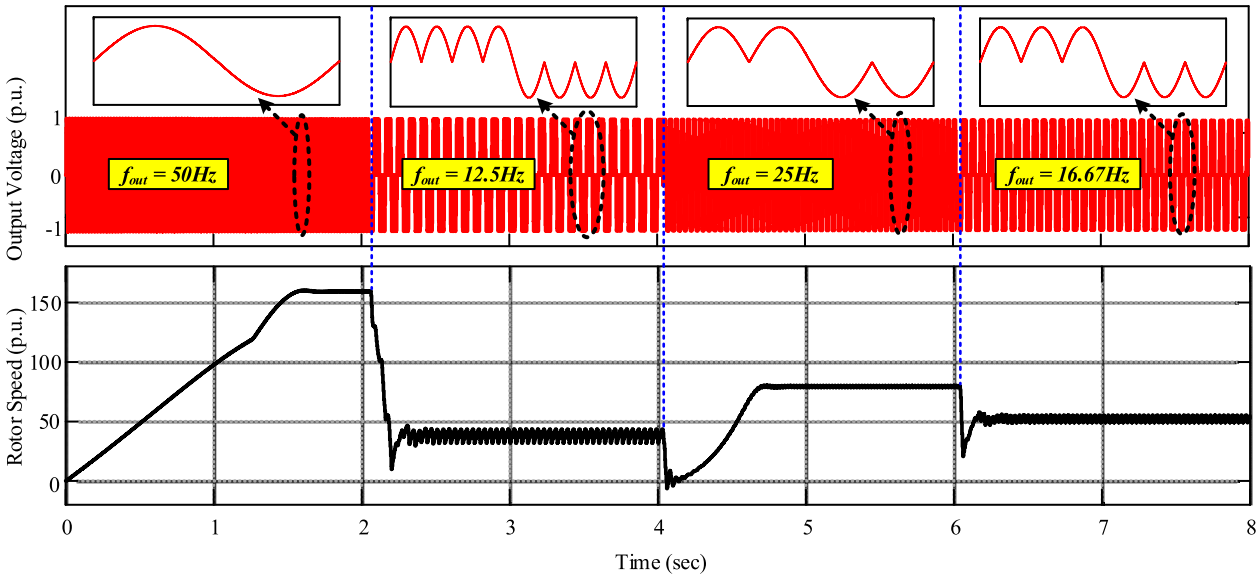

FIGURE 13. Rotor speed control of a single phase induction motor by operating the proposed converter as a step-down cycloconverter.

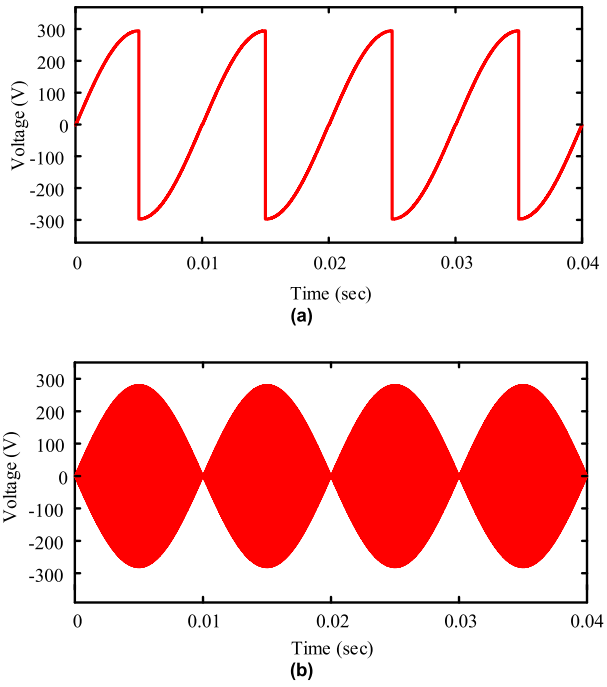

FIGURE 14. Output voltage of the proposed converter as a step-up cycloconverter, (a) 100Hz and (b) 20kHz.

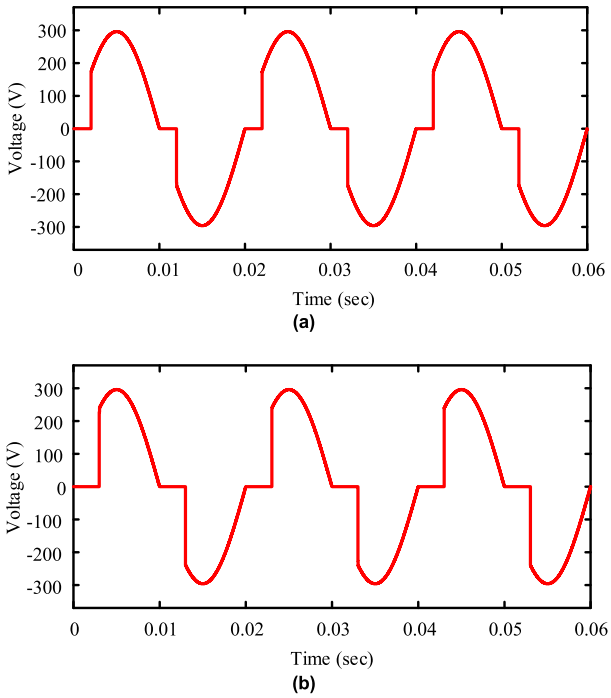

FIGURE 15. Output voltages of the proposed converter as an AC voltage regulator with delay angle, (a) $\alpha = 36^0$ and (b) $\alpha = 54^0$.

obtained as,

$$P_S = \sum_{m=1}^{N_{switch}} \left(P_{Sm\_on} + P_{Sm\_off}\right) \tag{45}$$

However, the proposed converter is operated at very low switching frequency with the off-state voltage close to zero volt for most of the applications which significantly decreases the switching losses. In case of induction heating, the switches are operated at very high frequency and the off-state voltage remains quite high which results in high switching loss. Nevertheless, by applying the above analysis, the two types of losses of the proposed multiconverter are measured at 2kW output power for all the energy conversion modes which are summarized in Fig. 10. From Fig. 10, it can be seen that the switching losses occurred during step-down cycloconverter mode are of very small amount

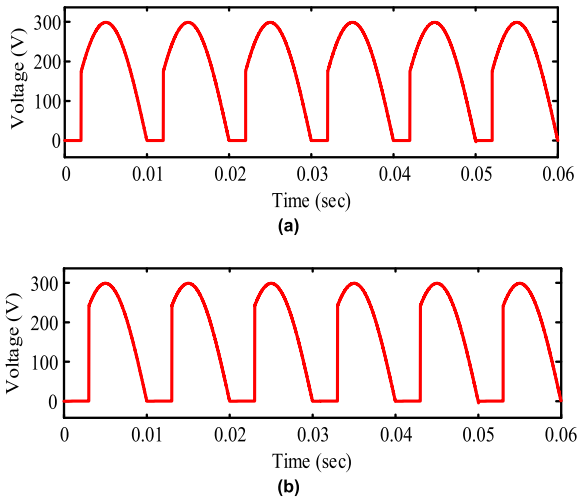

FIGURE 16. Output voltages of the proposed converter as a full wave controlled rectifier with control angle, (a) $\beta = 36^0$ and (b) $\beta = 54^0$.

where the conduction losses during this mode are higher as it consists of multiple states within a cycle of the output voltage. Moreover, there exist high switching losses during other energy conversion modes, as much switching is needed at high off-state voltage.

V. PERFORMANCE EVALUATION

In this section, performances of the proposed multiconverter are evaluated based on simulation results carried out in MATLAB/Simulink. However, the simulated results presented in accordance with the respective energy conversion mode for a certain application are as follows:

A. AS A STEP-DOWN CYCLOCONVERTER FOR ELECTRIC TRACTION

Generally, step-down cycloconverter is used to control the speed of electric traction motors in which the rotor speed varies with the input voltage frequency. In Fig. 11, the output voltage of the proposed converter as a step-down cycloconverter is represented where Fig. 11(a), Fig. 11(b) and Fig. 11(c) shows the output voltage of 25Hz, 16.67Hz, and 12.5Hz frequency respectively.

However, the responses of the proposed converter as a step-down cycloconverter during changing the output frequency dynamically are illustrated in Fig. 12. It is observed from Fig. 12 that the presented converter shows outstanding dynamic responses due to the utilization of soft switching elements at the time of changing output frequency randomly. Moreover, Fig. 13 represents the rotor speed control of a single phase induction motor with the variation in output frequency using the offered converter. Thus, it is obvious that the proposed converter is well suited for controlling the rotor speed of an electric traction motor.

B. AS A STEP-UP CYCLOCONVERTER FOR INDUCTION HEATING

In this subsection, the performance of the proposed converter as a step-up cycloconverter is validated with proper figures. The application area of a step-up cycloconverter includes induction heating, high frequency magnetic links etc. that require high frequency AC input voltage. Hence, in order increase the fed frequency, the presented converter can be used as a step-up cycloconverter as shown in Fig. 14 where the output voltage of 100Hz and 20kHz frequencies are depicted in Fig. 14(a) and Fig. 14(a) respectively.

C. AS AN AC VOLTAGE REGULATOR FOR VARIABLE AC POWER SUPPLY

In order to control the average and RMS value of the AC input voltage, the AC voltage regulators are used. The proposed converter is operated as an AC voltage regulator at the input frequency by varying the delay angle, α. Moreover, the converter uses soft switches, thus, the duty cycle is needed to determine with the help of the delay angle. In Fig. 15(a) and Fig. 15(b), the output voltages of the proposed converter with delay angle 36^0 and 54^0 are depicted respectively. Therefore, the proposed converter is also compatible as an efficient voltage regulator.

D. AS A FULL WAVE CONTROLLED RECTIFIER FOR VARIABLE DC POWER SUPPLY

In this subsection, the simulated results of the proposed converter as a controlled rectifier are illustrated in Fig. 16. The presented converter is able to act as a controlled rectifier using only one switch where it can be either S_1 switch or S_2 switch. However, the average and RMS output voltages of this rectifier are controlled using the predefined control angle, β. The output voltages of this full wave controlled rectifier with applied control angle 36^0 and 54^0 are represented in Fig. 16(a) and Fig. 16(b) respectively. Thus, the performance of the offered converter is also evaluated as a full wave controlled rectifier.

VI. EXPERIMENTAL VALIDATION

The theoretical background and the simulated results of the proposed multiconverter are verified in this section with experimental results obtained from the laboratory prototype developed in the lab. Fig. 17(a) exhibits the complete setup in the lab during experiment and the hardware prototype of the proposed multiconverter is shown in Fig. 17(b).

However, the prototype is made up of power MOSFETs (STP60NF06) and power diodes (1N5822), and a 12V stepped-down AC voltage produced by a center trapped transformer is used as input supply during experiment. In order to drive the gates of the switches, the switching signals are generated using Arduino Uno (ATMega16) processor board and then, they are boosted up through the driver circuits developed with optocouplers (TLP250) and isolated DC-DC converters (B1212s). Finally, the boosted pulses are applied to the gates of the switches using the synchronization mechanism offered by the zero-cross detector circuits, and then, the output voltages are recorded across resistive load on the oscilloscope screen. In Table 2, the list of equipment that is used during

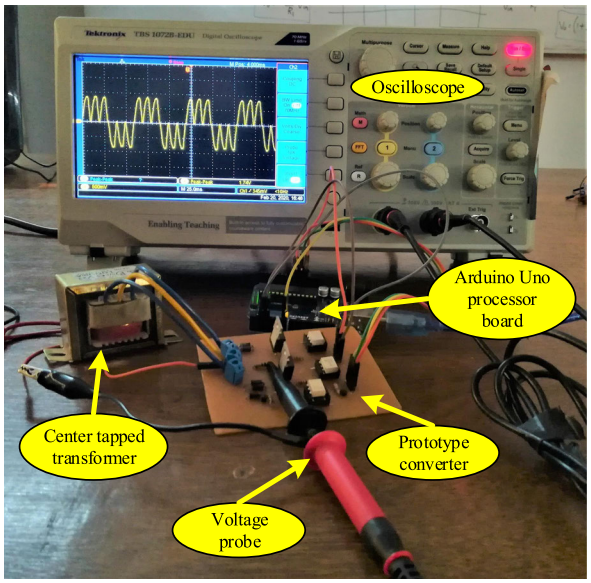

(a)

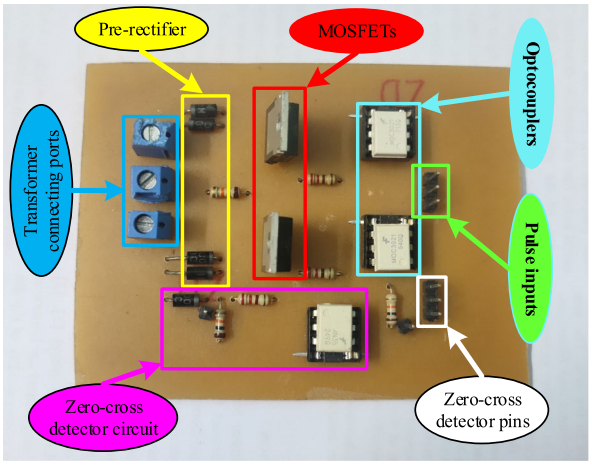

(b)

FIGURE 17. Experimental setup to verify the performance of the proposed multiconverter, (a) complete setup, and (b) magnified view of the prototype.

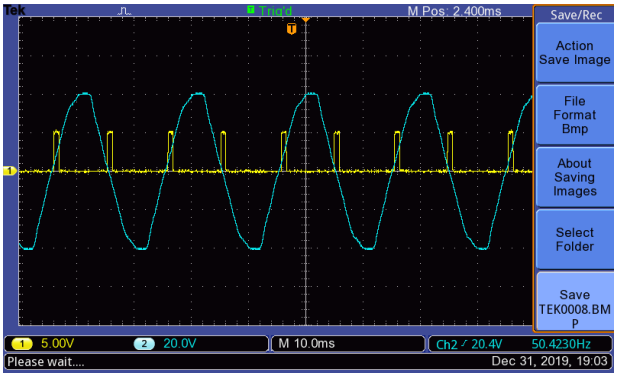

FIGURE 18. Performance verification of the zero-cross detector circuit before applying the gate pulses to the switches.

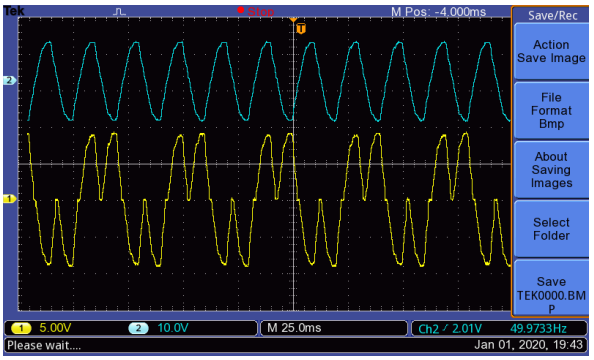

(a)

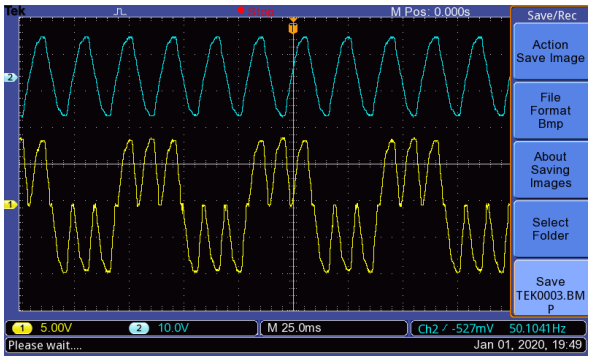

(b)

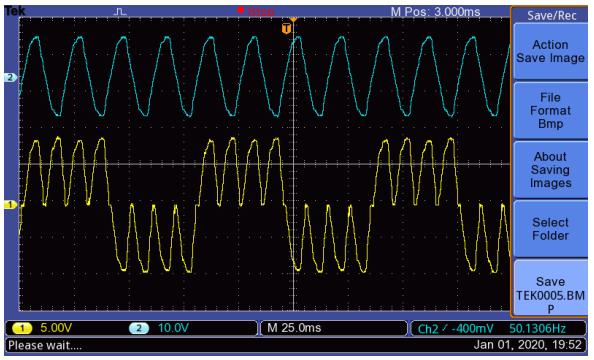

(c)

FIGURE 19. Input (blue) and output (yellow) voltages of the proposed prototype as a step-down cycloconverter with output frequency, (a) 25Hz, (b) 16.67Hz, and (c) 12.5Hz.

TABLE 2. List of equipment used during experiment.

Parameter Names	Model Names or Values
Input voltage	220V
Center tapped transformer	220V / 12V
MOSFET as switch	STP60NF06 (60V, 17A)
Power diode	1N5822 (40V, 3A)
Optocoupler/driver	4N35
Processor board	Arduino Uno (ATMega328p)
Oscilloscope	Tektronix

experiment is summarized. In Fig. 18, the performance of the zero-cross detector circuit is evaluated.

In order to validate the performance, the experimental results of the presented converter as a step-down cycloconverter are shown in Fig. 19. The output voltages of 25Hz, 16.67Hz, and 12.5Hz frequency are illustrated in Fig. 19(a), Fig. 19(b) and Fig. 19(c) respectively. Moreover, Fig. 20 represents the output voltage of 100Hz frequency

FIGURE 20. Input (blue) and output (yellow) voltages of the proposed prototype as a step-up cycloconverter with 100Hz output frequency.

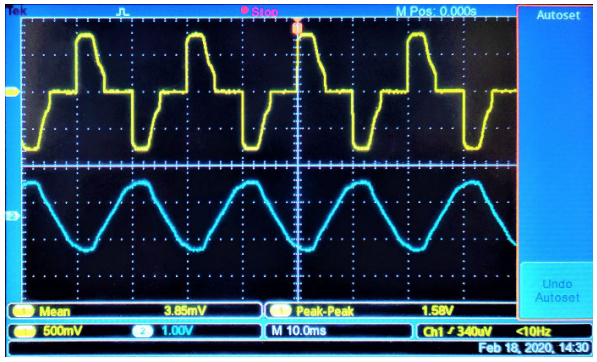

FIGURE 21. Input (blue) and output (yellow) voltages of the proposed prototype as an AC voltage regulator.

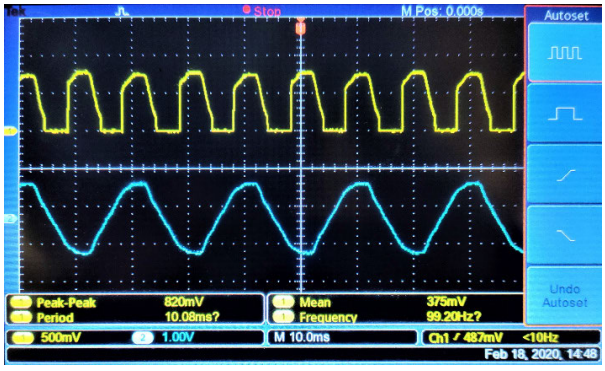

FIGURE 22. Input (blue) and output (yellow) voltages of the proposed prototype as a full wave controlled rectifier.

which also evaluates the performance of the converter for induction heating as a step-up cycloconverter experimentally. However, the input and output voltages of the prototype converter as an AC voltage regulator and full wave controlled rectifier are illustrated in Fig. 21 and Fig. 22 respectively. Therefore, it can be claimed that the proposed prototype shows quite similar results as compared to simulation results and it can be operated as a multiconverter. Moreover, it requires reduced number of semiconductor devices than the existing topologies that decreases the total equipment costs as well as total power losses and enhances the energy conversion efficiency. Hence, the proposed multiconverter is highly compatible for multiple applications including electric traction, induction heating, variable AC, and DC power supplies.

TABLE 3. Comparison of the proposed converter with existing converters.

Parameter Name	[33]	[32]	[34]	[35]	Proposed
Number of switches	10	8	8	6	2
Gate driver complexity	Very high	High	High	Medium	Very low
Costs of switches (p.u.)	1.0	0.8	0.8	0.6	0.2
Total losses	Very high	High	High	Medium	Very low
Galvanic Isolation availability	No	No	Yes	No	Yes
Equipment reliability	Low	Low	High	Low	High

VII. COMPARATIVE ANALYSIS

In this section, a comparative analysis of the proposed topology with some existing topologies is discussed in terms of some parameters including number of switching elements, gate driving complexity, total equipment costs, reliability, etc. The comparative studies among the topologies are summarized in Table 3 where it is seen that the proposed converter requires minimum number of switching elements to provide equivalent performance. Thus, the total equipment cost is significantly reduced than other topologies mentioned in Table 3. Moreover, the total losses occurred in the presented multiconverter are noticeably lower than the existing, as minimized number of semiconductor devices take part into conduction process. Therefore, the presented converter offers better energy conversion efficiency. Furthermore, the offered converter is applicable for multiple areas simultaneously which also indicates its superiority than the existing topologies.

VIII. CONCLUSION

In this paper, a new converter topology with reduced number of semiconductor switches has been proposed that has massive application areas including electric traction, induction heating, AC and DC variable power supply, etc. The circuit configuration, switching scheme, operating principle, and loss calculations of this converter have been explained sequentially in the above sections with necessary figures. In the later sections, the performances of the presented converter have been evaluated with both simulated and experimental results. At last, a comparative analysis of the proposed converter with some existing converters has been demonstrated. From the aforesaid analysis, it can be claimed that the proposed converter delivers some outstanding advantages such as (i) it requires reduced number of semiconductor

switches, (ii) it offers lower equipment costs, (iii) it produces lower losses than the existing topologies with enhanced energy conversion efficiency, (iv) it has a very low level of gate driver complexity and (v) it provides galvanic isolation that increases the equipment reliability as well as confirms safety

issues of the administrator. Therefore, it can be concluded that the proposed multiconverter is highly compatible with electric traction, induction heating, variable AC and DC power supplies, etc.

REFERENCES

[1] R. K. Surapaneni, D. B. Yelaverthi, and A. K. Rathore, "Cycloconverter-based double-ended microinverter topologies for solar photovoltaic AC module," *IEEE J. Emerg. Sel. Topics Power Electron.*, vol. 4, no. 4, pp. 1354–1361, Dec. 2016.

[2] D. Xu, S. Zhong, and J. Xu, "Bipolar phase shift modulation single-stage audio amplifier employing a full bridge active clamp for high efficiency low distortion," *IEEE Trans. Ind. Electron.*, early access, Jan. 23, 2020, doi: 10.1109/TIE.2020.2967727.

[3] Y. Liu, J. He, B. Ge, X. Li, Y. Xue, and F. Blaabjerg, "A simple space vector modulation of high-frequency AC linked three-phase-to-single-phase/DC converter," *IEEE Access*, vol. 8, pp. 59278–59289, 2020.

[4] K. H. Reddy, "PSO supported dual matrix converter for doubly fed induction generated driven by variable speed wind turbine system," *Int. J. Renew. Energy Res.*, vol. 10, no. 1, pp. 131–142, 2020.

[5] G. A. Alonso Orcajo, J. Rodriguez Diez, J. M. Cano, J. G. Norniella, J. F. P. Gonzalez, C. H. Rojas, P. Ardura G, and D. Cifrian R, "Enhancement of power quality in an actual hot rolling mill plant through a STATCOM," *IEEE Trans. Ind. Appl.*, vol. 56, no. 3, pp. 3238–3249, May 2020.

[6] M. T. S. Mahajan and M. V. Pawar, "Performance analysis of induction motor drive using SVPWM," *IJIRT*, vol. 6, no. 8, pp. 66–71, Jan. 2020.

[7] W. Ahmed, N. Ali, S. Nazir, and A. Khan, "Power quality improving based harmonical studies of a single phase step down bridge-cycloconverter," *J. Electr. Syst*, vol. 15, no. 1, pp. 109–122, 2019.

[8] I. A. Pires, R. A. Silva, I. T. O. Pereira, O. A. Faria, T. A. C. Maia, and B. D. J. C. Filho, "An assessment of immersion cooling for power electronics: An oil volume case study," *IEEE Trans. Ind. Appl.*, vol. 56, no. 3, pp. 3231–3237, May 2020.

[9] H. M. A. Antunes, I. A. Pires, and S. M. Silva, "Evaluation of series and parallel hybrid filters applied to hot strip mills with cycloconverters," *IEEE Trans. Ind. Appl.*, vol. 55, no. 6, pp. 6643–6651, Nov. 2019.

[10] H. F. Ahmed, H. Cha, A. A. Khan, and H.-G. Kim, "A novel buck–boost AC–AC converter with both inverting and noninverting operations and without commutation problem," *IEEE Trans. Power Electron.*, vol. 31, no. 6, pp. 4241–4251, Jun. 2016.

[11] S. Zhong, J. Xu, and X. Zhou, "2.1-channel switching amplifier with DC/high-frequency-AC mixed power supply for efficiency improvement and bus voltage pumping elimination," *IEEE Trans. Power Electron.*, vol. 33, no. 11, pp. 9110–9115, Nov. 2018.

[12] X. Zhou, J. Xu, and S. Zhong, "Single-stage soft-switching low-distortion bipolar PWM modulation high-frequency-link DC–AC converter with clamping circuits," *IEEE Trans. Ind. Electron.*, vol. 65, no. 10, pp. 7719–7729, Oct. 2018.

[13] B. Chen, B. Gu, L. Zhang, Z. U. Zahid, J.-S. Lai, Z. Liao, and R. Hao, "A high-efficiency MOSFET transformerless inverter for nonisolated microinverter applications," *IEEE Trans. Power Electron.*, vol. 30, no. 7, pp. 3610–3622, Jul. 2015.

[14] J. Nan, T. Hou-jun, L. Wei, and Y. Peng-sheng, "Analysis and control of buck-boost chopper type AC voltage regulator," in *Proc. IEEE 6th Int. Power Electron. Motion Control Conf.*, May 2009, pp. 1019–1023.

[15] G. Francisco Silva, T. Luis Moran, T. Miguel Torres, and V. Christian Weishaupt, "A method to evaluate cycloconverters commutation robustness under voltage and frequency variations in mining distribution systems," *IEEE Trans. Ind. Appl.*, vol. 54, no. 1, pp. 858–865, Jan. 2018.

[16] Y. Widjaja, "Method of operating semiconductor memory device with floating body transistor using silicon controlled rectifier principle," U.S. Patent 8 077 536, Dec. 13 2011.

[17] B.-K. Lee, J.-P. Kim, S.-G. Kim, and J.-Y. Lee, "An isolated/bidirectional PWM resonant converter for V2G(H) EV on-board charger," *IEEE Trans. Veh. Technol.*, vol. 66, no. 9, pp. 7741–7750, Sep. 2017.

[18] J. S. Vinodhini, R. S. R. Babu, and J. A. Glenn, "Single phase to single phase step-down cycloconverter for electric traction applications," in *Proc. Int. Conf. Electr., Electron., Optim. Techn. (ICEEOT)*, Mar. 2016, pp. 3647–4914.

[19] G. A. Orcajo, J. Rodriguez D., P. Ardura G., J. M. Cano, J. G. Norniella, R. Llera T., and D. Cifrian R., "Dynamic estimation of electrical demand in hot rolling mills," *IEEE Trans. Ind. Appl.*, vol. 52, no. 3, pp. 2714–2723, May 2016.

[20] L. Moran, C. A. Albistur, and R. Burgos, "Multimega VAR passive filters for mining applications: Practical limitations and technical considerations," *IEEE Trans. Ind. Appl.*, vol. 52, no. 6, pp. 5310–5317, Nov. 2016.

[21] D. Singh and R. G. Hoft, "Microcomputer-controlled single-phase cycloconverter," *IEEE Trans. Ind. Electron. Control Instrum.*, vol. IECI-25, no. 3, pp. 233–238, Aug. 1978.

[22] Y. Liu, G. T. Heydt, and R. F. Chu, "The power quality impact of cycloconverter control strategies," *IEEE Trans. Power Del.*, vol. 20, no. 2, pp. 1711–1718, Apr. 2005.

[23] D. R. Nayanasiri, D. M. Vilathgamuwa, and D. L. Maskell, "Half-wave cycloconverter-based photovoltaic microinverter topology with phase-shift power modulation," *IEEE Trans. Power Electron.*, vol. 28, no. 6, pp. 2700–2710, Jun. 2013.

[24] M.-K. Nguyen, Y.-G. Jung, and Y.-C. Lim, "Single-phase AC/AC buck-boost converter with single-phase matrix topology," in *Proc. 13th Eur. Conf. Power Electron. Appl.*, Sep. 2009, pp. 1–7.

[25] M. Kim, R. Lanclos, and R. S. Balog, "A PWM method for single-phase current-sourced high frequency AC link inverter," in *Proc. IEEE Texas Power Energy Conf. (TPEC)*, Feb. 2020, pp. 1–6.

[26] G. Seggewiss, J. Dai, and M. Fanslow, "Synchronous motors on grinding mills: The different excitation types and resulting performance characteristics with VFD control for new or retrofit installations," *IEEE Ind. Appl. Mag.*, vol. 21, no. 6, pp. 60–67, Nov. 2015.

[27] B. Wu, J. Pontt, J. Rodriguez, S. Bernet, and S. Kouro, "Current-source converter and cycloconverter topologies for industrial medium-voltage drives," *IEEE Trans. Ind. Electron.*, vol. 55, no. 7, pp. 2786–2797, Jul. 2008.

[28] Y. Hirane and W. Shepherd, "Theoretical assessment of a variable-frequency envelope cycloconverter," *IEEE Trans. Ind. Electron. Control Instrum.*, vol. IECI-25, no. 3, pp. 238–246, Aug. 1978.

[29] B.-H. Kwon, B.-D. Min, and J.-H. Kim, "Novel topologies of AC choppers," *IEE Proc.-Electr. Power Appl.*, vol. 143, no. 4, pp. 323–330, Jul. 1996.

[30] X. P. Fang, Z. M. Qian, and F. Z. Peng, "Single-phase Z-source PWM AC-AC converters," *IEEE Power Electron. Lett.*, vol. 3, no. 4, pp. 121–124, Dec. 2005.

[31] T. B. Lazzarin, R. Andersen, and I. Barbi, "A switched-capacitor three-phase AC-AC converter," *IEEE Trans. Ind. Electron.*, vol. 62, no. 2, pp. 735–745, Feb. 2015.

[32] C.-M. Young, H.-L. Chen, and M.-H. Chen, "A Cockcroft–Walton voltage multiplier fed by a three-phase-to-single-phase matrix converter with PFC," *IEEE Trans. Ind. Appl.*, vol. 50, no. 3, pp. 1994–2004, May 2014.

[33] M.-K. Nguyen, Y.-G. Jung, Y.-C. Lim, and Y.-M. Kim, "A single-phase Z-source buck–boost matrix converter," *IEEE Trans. Power Electron.*, vol. 25, no. 2, pp. 453–462, Feb. 2010.

[34] M. Kumar, P. Agarwal, and V. Agarwal, "A novel soft switched cycloinverter," *IEEE Trans. Ind. Electron.*, vol. 62, no. 1, pp. 153–162, Jan. 2015.

[35] H. F. Ahmed, H. Cha, A. A. Khan, J. Kim, and J. Cho, "A single-phase buck–boost matrix converter with only six switches and without commutation problem," *IEEE Trans. Power Electron.*, vol. 32, no. 2, pp. 1232–1244, Feb. 2017.

[36] M. H. Rashid, *Power Electronics Handbook*. London, U.K.: Butterworth, 2017.

[37] M. H. Mondol, M. R. Tur, S. P. Biswas, M. K. Hosain, S. Shuvo, and E. Hossain, "Compact three phase multilevel inverter for low and medium power photovoltaic systems," *IEEE Access*, vol. 8, pp. 60824–60837, 2020.

[38] A. Taghvaie, J. Adabi, and M. Rezanejad, "A self-balanced step-up multilevel inverter based on switched-capacitor structure," *IEEE Trans. Power Electron.*, vol. 33, no. 1, pp. 199–209, Jan. 2018.

MD. HALIM MONDOL was born in Meherpur, Bangladesh, in 1996. He is currently pursuing the B.Sc. degree in electronics and telecommunication engineering (ETE) with the Faculty of Electrical and Computer Engineering, Rajshahi University of Engineering and Technology (RUET), Rajshahi, Bangladesh. He has been working in the area of power electronics converter for renewable energy conversion and distribution for the last two years. He has published a number of research articles in this field. His current research interests include modeling, analysis, design, and control of power electronic converters; renewable energy conversion technologies; control systems; and isolated dc micro grid. He received the Dr. M. H. Rashid Best Paper Award at ICECTE for his tremendous research, in 2019.

MD. SHIHAB UDDIN was born in Jashore, Bangladesh, in 1997. He is currently pursuing the B.Sc. degree in electronics and telecommunication engineering (ETE) with the Faculty of Electrical and Computer Engineering, Rajshahi University of Engineering and Technology (RUET), Rajshahi, Bangladesh. His current research interests include power electronics devices, renewable energy systems, microcontroller programming and embedded system, and smart micro-grids.

EKLAS HOSSAIN (Senior Member, IEEE) received the B.S. degree in electrical and electronic engineering from the Khulna University of Engineering and Technology, Bangladesh, in 2006, the M.S. degree in mechatronics and robotics engineering from the International Islamic University of Malaysia, Malaysia, in 2010, and the Ph.D. degree from the College of Engineering and Applied Science, University of Wisconsin Milwaukee (UWM). He has been working in the area of distributed power systems and renewable energy integration for the last ten years. He has published a number of research articles and posters in this field. He has been involved with several research projects on renewable energy and grid-tied microgrid system at Oregon Tech, as an Assistant Professor with the Department of Electrical Engineering and Renewable Energy, since 2015. He is working as an Associate Researcher with the Oregon Renewable Energy Center (OREC). He is also a registered Professional Engineer (PE) in the state of Oregon, USA. He is also a Certified Energy Manager (CEM) and Renewable Energy Professional (REP). His research interests include modeling, analysis, design, and control of power electronic devices; energy storage systems; renewable energy sources; integration of distributed generation systems; microgrid and smart grid applications; robotics, and advanced control systems. Dr. Hossain, with his dedicated research team, is looking forward to explore methods to make the electric power systems more sustainable, cost-effective, and secure through extensive research and analysis on energy storage, microgrid systems, and renewable energy sources. He is the Senior Member of Association of Energy Engineers (AEE). He is the winner of the Rising Faculty Scholar Award, in 2019, from the Oregon Institute of Technology for his outstanding contribution in teaching. He is serving as an Associate Editor for IEEE Access.

SHUVRA PROKASH BISWAS received the B.Sc. degree in electronics and telecommunication engineering (ETE) from the Rajshahi University of Engineering and Technology (RUET), Rajshahi, Bangladesh, in 2017. He is currently a Lecturer with the Department of ETE, RUET. He has been working in the area of advanced power electronics converter for distributed power systems and industrial drives for the last four years. He has published a number of research articles and posters in this field. His research interests include power electronics, electrical machines and drives, control systems, renewable energy systems, real time hardware-in-the-loop (HIL) simulations, and smart micro-grids.